

Evolutionary Transition toward Defective RNAs That Are Infectious by Complementation

Juan García-Arriaza,¹ Susanna C. Manrubia,² Miguel Toja,^{1†} Esteban Domingo,^{1*}
and Cristina Escarmís¹

*Centro de Biología Molecular “Severo Ochoa” (CSIC-UAM), Universidad Autónoma de Madrid, Cantoblanco,¹
and Centro de Astrobiología (CSIC-INTA), Torrejón de Ardoz,² Madrid, Spain*

Received 4 March 2004/Accepted 14 June 2004

Passage of foot-and-mouth disease virus (FMDV) in cell culture resulted in the generation of defective RNAs that were infectious by complementation. Deletions (of nucleotides 417, 999, and 1017) mapped in the L proteinase and capsid protein-coding regions. Cell killing followed two-hit kinetics, defective genomes were encapsidated into separate viral particles, and individual viral plaques contained defective genomes with no detectable standard FMDV RNA. Infection in the absence of standard FMDV RNA was achieved by cotransfection of susceptible cells with transcripts produced in vitro from plasmids encoding the defective genomes. These results document the first step of an evolutionary transition toward genome segmentation of an unsegmented RNA virus and provide an experimental system to compare rates of RNA progeny production and resistance to enhanced mutagenesis of a segmented genome versus its unsegmented counterpart.

Mutation, recombination, and ensuing phenotypic modifications in response to selective pressures can be readily observed and quantitated with RNA viruses both in cell culture and in vivo within modest time periods. This has rendered viruses suitable experimental systems for studies of basic Darwinian processes of genetic modification, competition, and selection or random drift as agents of genome diversification and biological adaptation (reviewed in references 1, 8, and 12). However, some major evolutionary transitions such as RNA genome segmentation have never been observed in the laboratory, yet they have probably occurred, given the hundreds of animal, plant, bacterial, and fungal viruses with segmented RNA genomes that have been described, including picornavirus-like plant RNA viruses (43). We have carried out extensive studies on the population dynamics of the important animal picornavirus foot-and-mouth disease virus (FMDV), including that of phenotypic evolution upon long-term serial cytopathic infections of BHK-21 cells (2). Unexpectedly, after more than 200 serial infections of viral population C-S8c1 of FMDV (a clone of serotype C [reviewed in reference 33]), defective genomes became dominant in the population. Defective interfering (DI) particles are frequently produced upon passage of RNA viruses at a high multiplicity of infection (MOI). DI particles are deletion mutants that require the presence of helper virus for replication and can interfere with the replication of the standard infectious virus (14–16, 29, 32, 35). The results described here show that defective genomes which individually could not cause cytopathology could nevertheless complement each other to produce progeny and kill cells in the absence of standard virus. The results provide, to our knowledge, the first description of defective RNA genomes occurring

during viral replication that can be stably maintained by complementation upon passage at a high MOI in the absence of standard infectious virus. Therefore, the results provide experimental evidence of the initial step of an evolutionary transition towards genome segmentation of an unsegmented RNA virus.

MATERIALS AND METHODS

Cells, viruses, and infections. The origin of baby hamster kidney 21 (BHK-21) cells and procedures for cell growth, infection of cell monolayers with foot-and-mouth disease virus (FMDV) in liquid medium, and for plaque assays in semi-solid agar medium have been previously described (3, 9, 38). FMDV C-S8c1 is a plaque-purified virus of the European serotype C, natural isolate C₁ Santa-Pau Spain 70 (38). FMDV C-S8p260 is a viral population obtained after 260 serial cytopathic passages of C-S8c1 at high MOIs in BHK-21 cells (2×10^6 BHK-21 cells infected with the virus contained in 200 μ l of the supernatant from the previous infection). FMDV C-S8p260p3d is a viral population obtained after three serial cytopathic passages of C-S8p260 at low MOIs in BHK-21 cells (2×10^6 BHK-21 cells infected with 200 μ l of a 10^{-3} dilution of the supernatant from the previous infection). FMDV MARLS is a monoclonal antibody escape mutant obtained from FMDV C-S8c1 passaged 213 times in BHK-21 cells (6). The fitness of FMDV C-S8p260p3d and MARLS relative to C-S8c1 is 70 and 130, respectively (28; J. García-Arriaza, unpublished results).

Cell killing assay. Cell killing was quantified essentially as previously described (36) and consisted in determining the minimum number of viral particles required to kill 10^4 BHK-21 cells after variable times of infection. The cells were infected with serial dilutions of the viruses to be tested (the number of viral particles added was determined by real-time PCR with a LightCycler [Roche] instrument), and at different times postinfection cell monolayers were fixed with 2% formaldehyde and stained with 2% crystal violet in 2% formaldehyde.

FMDV purification. FMDV particles were purified as previously described (7). Briefly, virus was concentrated through a sucrose cushion and then resuspended in TNE (0.1 M Tris [pH 7.5], 0.05 M EDTA, 0.5 M NaCl) and sedimented through a sucrose gradient (7.5 to 30% in TNE). Fractions of 700 μ l were collected for analysis.

Quantification of viral particles by electron microscopy. Purified virus was mixed with an equal volume of a solution of latex beads (91-nm diameter; 1.37×10^{12} latex beads/ml) (Balzers Union). The samples were adsorbed for 2 to 3 min to copper grids coated with collodion-carbon and ionized. The grids were then fixed with 2% glutaraldehyde, negatively stained with 2% uranyl acetate, and air dried. The grid was observed in a transmission electron microscope (JEM1010; Jeol, Tokyo, Japan), and the numbers of viral particles and latex beads were counted in multiple, independent images. The number and size of particles were

* Corresponding author. Mailing address: Centro de Biología Molecular “Severo Ochoa” (CSIC-UAM), Universidad Autónoma de Madrid, Cantoblanco, Madrid 28049, Spain. Phone: 34 91 4978485. Fax: 34 91 4974799. E-mail: edomingo@cbm.uam.es.

† Present address: Operon S.A., 50419-Cuarte de Huerva, Zaragoza, Spain.

determined, and standard deviations were calculated, as detailed in Results (see also Fig. 3C).

RNA quantification, cDNA synthesis, PCR amplification, and nucleotide sequencing. Viral RNA was extracted from supernatants of infected cells, purified virus, or individual viral plaques by treatment with Trizol (Invitrogen) as previously described (37). RNA quantification was performed by real-time PCR by using the LightCycler instrument with the LightCycler RNA Master SYBR Green I kit or LightCycler RNA Amplification SYBR Green I kit (both from Roche) for small (<500 bp) or large (>500 bp) DNA fragments, respectively. Reverse transcription (RT) was carried out by using avian myeloblastosis virus reverse transcriptase (Promega), and PCR amplification was performed by using either Ampli-Taq polymerase (Perkin-Elmer) or an Expand High Fidelity DNA polymerase system (Roche), as specified by the manufacturers. Amplification products were analyzed by 1% agarose gel electrophoresis and ethidium bromide staining. Nucleotide sequencing was carried out as previously described (10, 11). The positions of the primers in the FMDV genome will be given upon request (the GenBank accession number for the C-S8c1 genomic sequence is AJ133357 [42]).

Construction of an infectious clone of FMDV C-S8c1 and of derivatives containing defective genomes. An infectious clone of FMDV C-S8c1 was constructed by recombining subclones that represented the whole genome except the poly(C) tract (41) into a pGEM-1 plasmid under the control of the SP6 promoter. A short poly(C) tract was obtained from the genomic RNA by amplification of a 561-nucleotide DNA fragment with Vent DNA polymerase by using 76°C as the hybridization and elongation temperature. A unique NdeI site was introduced at the 3' end of the viral genome after a six adenylates tract. The clone was optimized by eliminating three C residues located between the SP6 promoter and the FMDV sequence, increasing the poly(C) tract length to 35 Cs and increasing the 3'-terminal poly(A) length from 6 to 25 residues. This infectious clone is named pMT28 and the specific infectivity of its transcript is 10^5 PFU/ μ g of RNA. Plasmids pMT Δ 417 and pMT Δ 999 were constructed by substituting the region spanning nucleotides 436 to 4201 of pMT28 with the corresponding region from the defective genomes Δ 417 and Δ 999, respectively. The restriction sites used for the construction were HpaI (position 436) and BglII (position 4201) present in pMT28 as unique recognition sites. Procedures for the purification of plasmids, transformation of *Escherichia coli* DH5 α competent cells, and isolation of bacterial colonies have been previously described (3, 37).

In vitro RNA transcription and cell transfection. Plasmids including FMDV cDNA with deletions (pMT Δ 417 and pMT Δ 999) were linearized at the NdeI site, and RNA transcription by SP6 polymerase was performed as previously described (3). BHK-21 cells were transfected with RNA transcripts by electroporation, as previously described (3, 17). Briefly, 0.5 ml of BHK-21 cells at a concentration of 10^6 to 10^7 cells/ml were mixed with 12 μ g of RNA in a 4-mm cuvette. The cells were then pulsed twice at 280 V, 400 Ω of resistance, and a capacitance of 250 μ F, with a Bio-Rad Gene Pulser. After electroporation the cells were allowed to attach to tissue culture plates in the presence of Dulbecco's modified Eagle's medium supplemented with 10% fetal calf serum. The dead cells and medium were removed after 4 h, and fresh medium with 2% fetal calf serum was added to the cultures, followed by incubation at 37°C.

RESULTS

Defective genomes in a multiply passaged FMDV population. Clone FMDV C-S8c1 was serially passaged at high MOIs in BHK-21 cells, and at passage 143 (population termed C-S8p143) a defective genome dependent on helper, standard FMDV, was detected in the viral population (6). To investigate the evolution of this defective genome, the virus was further passaged at high MOIs, and at passage 260 (population C-S8p260) viral RNA was extracted from the culture medium and analyzed. C-S8p260 RNA was amplified by RT-PCR by using different pairs of primers which covered the entire C-S8c1 genome (Fig. 1A and B). Amplifications that spanned the L protease- and capsid-coding regions detected three RNA molecules smaller than the standard C-S8c1 genome, suggesting the presence of genomes with deletions. Nucleotide sequencing identified three classes of deletions. One class of RNA contained a deletion of 417 nucleotides within the L protease-coding region, and two other classes of RNA con-

tained deletions of 999 or 1,017 nucleotides in the capsid-coding region. These RNAs are termed Δ 417, Δ 999, and Δ 1017, respectively. The Δ 417 deletion involves positions 1153 to 1571 (FMDV genome numbering follows the method of reference 10), and it was already present in C-S8p143 (6). The Δ 999 deletion spans positions 2793 to 3793, and Δ 1017 spans positions 1932 to 2950 (Fig. 1A). Deletions Δ 999 and Δ 1017 overlap by 156 nucleotides. The deletions did not alter the open reading frame of the aphthovirus genome. The presence of these three classes of deletions was confirmed by using different independent preparations of RNA from C-S8p260 as template. No RNA molecules containing more than one deletion were detected.

To determine the relative abundance of RNA of standard size and RNA with deletions in C-S8p260, the different classes of RNA were quantified by real-time PCR (LightCycler) by using different pairs of primers specific for each genome class (Table 1). In C-S8p260 there was the same amount of Δ 417, Δ 999, and Δ 1017 RNA estimated in 10^5 RNA molecules per infected cell, and no standard RNA was detected. Amplifications of serial dilutions of a standard RNA indicated that in C-S8p260 there was at least 10,000 times less standard FMDV RNA than genomes with deletions. To rescue standard genomes that could be present in the population, C-S8p260 was serially passaged three times at low MOIs to yield preparation C-S8p260p3d which contained standard size genomes and no RNAs with deletions (Fig. 1A and B). This result suggests that the genomes with deletions are defective and that standard genomes were present as a minority in C-S8p260.

Viral production by FMDV C-S8p260 and C-S8p260p3d. Many infections of approximately 10^4 viral particles per cell indicated that viral production in infections with C-S8p260 was consistently lower (average of 0.97 ± 0.78 PFU/cell) than with C-S8p260p3d (average of 187 ± 96 PFU/cell) (each value is the average of at least 15 determinations). Despite the lower yield, C-S8p260 produced complete cytopathology at approximately the same time as C-S8p260p3d (6 to 9 h postinfection). The plaque size for C-S8p260 and C-S8p260p3d on BHK-21 cell monolayers was 0.94 ± 0.53 and 2.68 ± 0.86 mm, respectively (average of measurements of 100 plaques) (Fig. 1C). These data indicate differences in the capacity to produce viral progeny of C-S8p260 and C-S8p260p3d, despite producing a similar cytopathology.

Particles with defective RNAs form plaques on BHK-21 cell monolayers. Viral populations C-S8p260 and C-S8p260p3d were plated on BHK-21 monolayers, and single plaques were isolated. The nature of the RNAs contained in the individual plaques was analyzed by RT-PCR (Table 2). A total of 61 of 62 plaques obtained from C-S8p260 contained Δ 417 and Δ 999 or Δ 1017 RNA and no detectable standard RNA. Some of these plaques were obtained from a second or a third replating. This result strongly suggests that the cytopathology associated with plaque formation was produced by RNAs containing deletions, in the absence of standard RNA. As expected, C-S8p260p3d yielded only plaques containing virus with standard size genomes. One out of 42 plaques isolated from a first plaque assay of C-S8p260 contained a standard genome as its only genome. This result again indicates the existence of standard length genomes as a minority in population C-S8p260, which upon

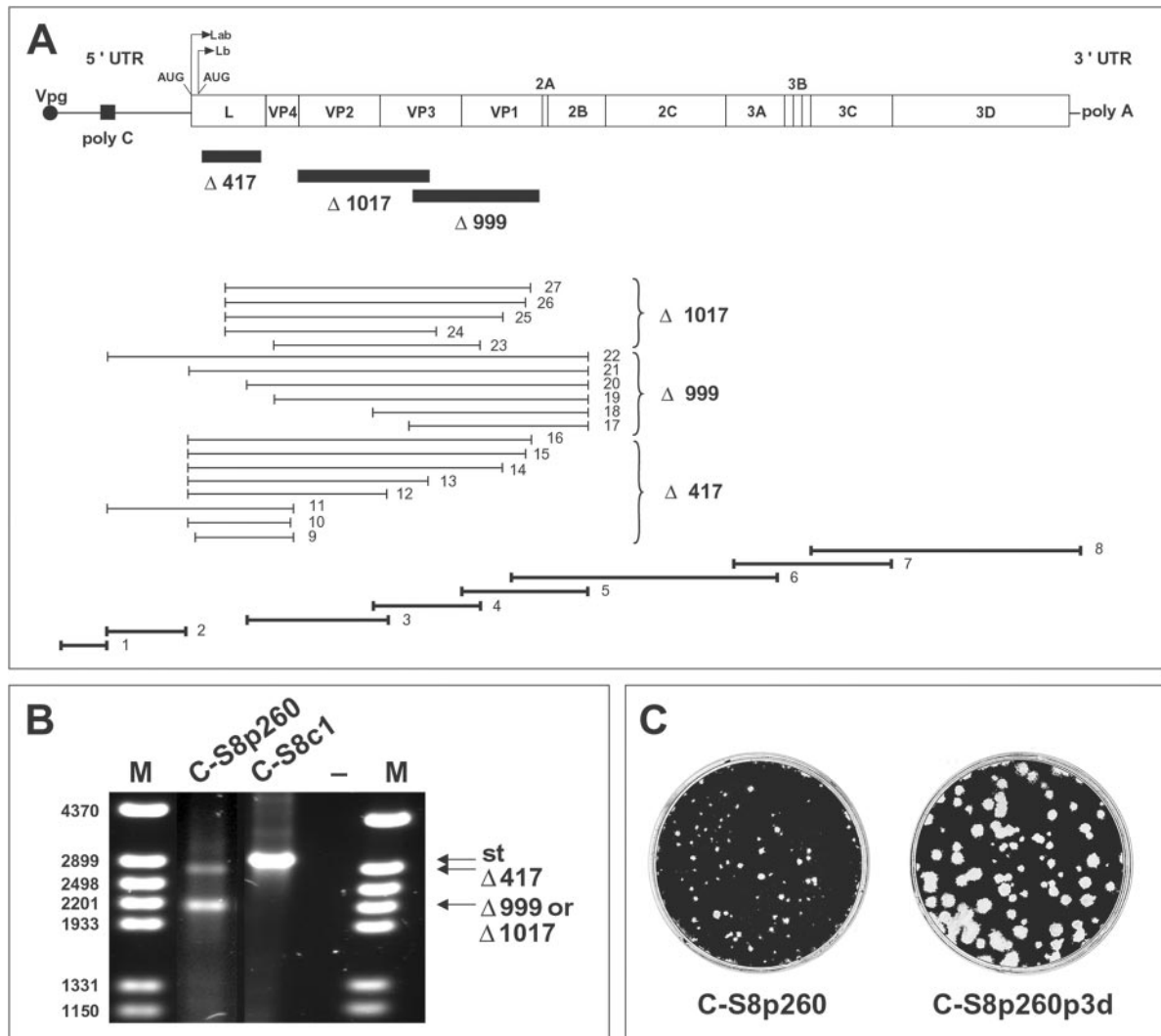


FIG. 1. RT-PCR amplifications used to detect defective genomes in FMDV population C-S8p260. (A) Map of the 8,115 residues of the FMDV C-S8c1 genome, excluding the internal polyribocytidylate [poly(C)] and the 3' end poly(A) (4, 10, 42). Lines indicate noncoding regions, including the 5' untranslated region (5' UTR) containing the poly(C) tract and the 3' untranslated region (3' UTR) with the terminal poly(A) tract; boxes delimit protein-coding regions. Two functional initiation AUG codons give rise to two forms of the L protease, Lab and Lb. Filled rectangles below the map indicate the position of deletions $\Delta 417$, $\Delta 999$, and $\Delta 1017$. The thin lines below the map show the RT-PCR amplification products, covering the C-S8p260 genome, used to map RNA deletions (the major class of deletion detected is indicated on the right). The location in the FMDV C-S8c1 genome of the primers used will be given upon request. RT-PCR amplifications that resulted only in DNA fragments of standard length are depicted as thick lines at the bottom of the scheme. The same RT-PCR amplifications, covering the C-S8p260p3d genome, did not detect any deletion. (B) Agarose gel showing one representative RT-PCR amplification (panel A, number 21) obtained from C-S8p260. The DNA products corresponding to standard (st) size RNA and RNAs with deletions are indicated by an arrow on the right. The DNA products obtained from C-S8p260p3d are indistinguishable from that obtained from C-S8c1. Lane M, molecular size markers (HindIII-digested $\phi 29$ DNA; the corresponding sizes [base pairs] are indicated on the left); lane -, negative control without RNA. (C) Plaque size produced by virus C-S8p260 and C-S8p260p3d. Confluent BHK-21 cell monolayers (2×10^6 to 4×10^6 cells per 20 cm^2) were infected with serial dilutions of FMDV C-S8p260 or C-S8p260p3d, and at 24 h postinfection cell monolayers were fixed with 2% formaldehyde and stained with 2% crystal violet in 2% formaldehyde. The average diameter of the plaques produced by C-S8p260 was approximately three times smaller than that of plaques produced by C-S8p260p3d, as described in the text. Procedures for plaque assay in semisolid agar medium are described in Materials and Methods.

three serial passages at low MOIs originated population C-S8p260p3d, which is devoid of detectable defective genomes.

Cell killing by C-S8p260 and C-S8p260p3d. An FMDV cell killing assay for BHK-21 cells (reference 36 and Materials and Methods) revealed a very significant difference in the behavior of FMDV populations C-S8p260 and C-S8p260p3d (Fig. 2). The time needed to kill 10^4 cells depended logarithmically on the number of viral particles added for C-S8p260p3d, MARLS,

and C-S8c1 (the latter two FMDV variants, described in Materials and Methods, were included to control the effect of relative fitness on cell killing). However, for C-S8p260, such dependence was a power-law function. A theoretical model (unpublished data) that relates the time needed for cell killing (T), the initial number of viral particles (n_0), and the fraction of infectious particles produced after a replication cycle (in a single cell) which can effectively infect new cells, indicates a

TABLE 1. Quantification of different RNAs present in C-S8p260 and C-S8p260p3d

Amplification no. ^a	Position of primers ^b		Size of expected product (bp)	Quantified RNAs ^c	No. of RNA molecules/ μ l ^d	
	Sense	Antisense			C-S8p260	C-S8p260p3d
28	5344–5363	5699–5678	356	total RNA	$2.1 \pm 0.6 \times 10^8$	$3.2 \pm 0.8 \times 10^8$
29	1539–1560	2926–2903	1388	st	$<1.7 \pm 0.4 \times 10^{4e}$	$1.7 \pm 0.4 \times 10^8$
30	2744–2770	2926–2903	183	st + Δ 417	$1.3 \pm 0.1 \times 10^8$	$1.7 \pm 0.4 \times 10^8$
31	1305–1330	2140–2122	836	st + Δ 999	$8.5 \pm 3.4 \times 10^7$	$2.2 \pm 0.9 \times 10^8$
32	1539–1560	2983–2961	1445 + 429	st + Δ 1017	$8.2 \pm 5.8 \times 10^7$	$5.8 \pm 4.8 \times 10^8$
33	1692–1710	2140–2122	449	st + Δ 417 + Δ 999	$2.2 \pm 0.6 \times 10^8$	$2.6 \pm 0.6 \times 10^8$
34	3175–3194	3518–3496	344	st + Δ 417 + Δ 1017	$1.6 \pm 0.2 \times 10^8$	$2.6 \pm 0.8 \times 10^8$
35	1305–1330	1619–1596	315	st + Δ 999 + Δ 1017	$9.8 \pm 2.4 \times 10^7$	$1.9 \pm 0.6 \times 10^8$

^a Amplifications were carried out with primers that could amplify specifically each class of RNA. Numbers are correlative to those of the amplifications shown in Fig. 1A.

^b Position refers to the FMDV C-S8c1 genome, with the numbering used in reference 10.

^c Class of RNA quantified by the specific primers. In C-S8p260p3d (free of defective genomes), all the amplifications quantified only standard (st) genomes.

^d Number of RNA molecules per microliter of supernatant of infected cells. 10^8 RNA molecules/ μ l corresponds to about 10^5 molecules per infected cell. Each value is the average of at least two independent determinations and represents the mean of triplicate amplification assays; standard deviations are indicated.

^e No standard RNA was detected in C-S8p260 by real-time PCR (Light Cycler). To ensure that standard (st) RNA could be amplified in the presence of an excess of RNAs with deletions amplifications with primers located within the sequences deleted in Δ RNAs (amplification number 29) were carried out with a fixed amount of C-S8p260 RNA (corresponding to 1 μ l [\approx 3.4 ng RNA] of an undiluted RNA preparation extracted from C-S8p260) and 10-fold serial dilutions of C-S8p260p3d (corresponding to RNA extract from C-S8p260p3d). Standard RNA was detected even when present at a 10^{-4} dilution relative to Δ RNAs; the intensity of the RT-PCR band was about 50% of the intensity observed in the absence of RNAs with deletions. Since the last dilution of C-S8p260p3d in which there was positive amplification was 10^{-4} , in C-S8p260 the maximum amount of st RNA was 1.7×10^4 molecules per μ l of supernatant of infected cells.

logarithmic function of T versus n_o when a single particle is sufficient to kill a cell and a power-law function when two (or more) particles are needed to kill a cell, in agreement with the experimental results. Therefore, in C-S8p260 two particles with defective RNAs are needed to initiate infection of a single cell, suggesting that infection is produced by complementation of the two defective RNAs. The need for complementation provides an interpretation of the fact that the yield of C-S8p260 (measured as PFU/cell) was consistently about 200-fold lower than the yield of C-S8p260p3d, despite a similar time of appearance of cytopathology (see above). Therefore, there is an ambiguity in the definition of PFU in such a complementation system.

Complementation of RNA transcripts containing deletions Δ 417 and Δ 999 in the absence of standard RNA. To prove that Δ 417 and Δ 999 RNAs can infect by complementation, BHK-21 cells were transfected with either Δ 417 RNA, Δ 999 RNA, or the two RNAs together. The RNAs were transcribed from plasmids pMT Δ 417 and pMT Δ 999. The presence or absence of cytopathology of transfected cells was monitored, and samples

of cell culture supernatants at different times posttransfection were analyzed for the presence of defective RNAs or standard RNAs and for infectivity (Table 3). Each Δ 417 or Δ 999 RNA transcript alone failed to produce cytopathology of BHK-21 cells at 5 days posttransfection. Nor was cytopathology observed upon blind infection of BHK-21 cells with supernatants

TABLE 2. Detection of defective and standard genomes in virus from plaques formed by C-S8p260 and C-S8p260p3d

Virus and assay ^a	No. of plaques analyzed	Genomes present in the analyzed plaques ^b		
		st	Δ 417	Δ 999 or Δ 1017
C-S8p260				
First plaque assay	41	–	+	+
	1	+	–	–
Second plaque assay	17	–	+	+
Third plaque assay	3	–	+	+
C-S8p260p3d plaque assay	5	+	–	–

^a The origin of C-S8p260 and C-S8p260p3d and the procedure for the plaque assays are described in Materials and Methods. Three serial plaque assays were done with various plaques from C-S8p260.

^b RT-PCR amplifications used were numbers 9, 10, 13, and 21, to detect Δ 417 and 17, 18, 20, and 21, to detect Δ 999 or Δ 1017 (Fig. 1A); amplification number 29 shown in Table 1 was used to detect standard (st) RNA.

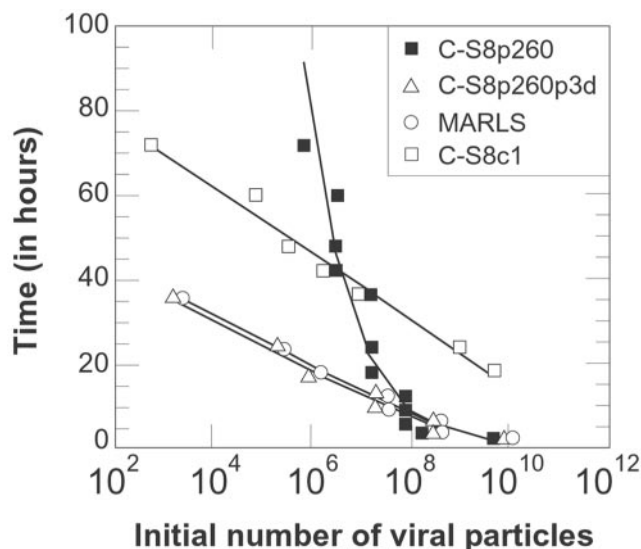


FIG. 2. Killing of BHK-21 cells by FMDV C-S8p260, C-S8p260p3d, MARLS, and C-S8c1. Time needed to kill 10^4 BHK-21 cells as a function of the initial number of viral particles added. One representative experiment of four is shown. For standard viruses (open symbols) the time T required to produce complete cell killing is a logarithmic function of the initial number of viral particles n_o . Least square fits to the experimental data (continuous lines) yielded the following functions: for C-S8p260p3d, $T = -2.35 \ln(n_o) + 51.8$, with a regression coefficient $r^2 = 0.96$; for MARLS, $T = -2.34 \ln(n_o) + 52.4$, $r^2 = 0.96$; for C-S8c1, $T = -3.41 \ln(n_o) + 93.3$, $r^2 = 0.98$. For the defective RNAs containing viral population C-S8p260 (solid symbols), the time T follows instead a power-law function, such that $\ln(T) = \ln(44844) - 0.46 \ln(n_o)$, with $r^2 = 0.91$.

TABLE 3. Complementation of defective RNA transcripts from pMTΔ417 and pMTΔ999

Parameter	RNA at times post-transfection ^a									
	pMTΔ417 + pMTΔ999								pMTΔ417	pMTΔ999
	0 h	2 h	4 h	16 h	24 h	36 h	72 h	5 days	5 days	5 days
Cytopathology ^b	–	–	–	–	–	–	–	+	–	–
RT-PCR of RNA from transfection supernatants ^c	Δ417, Δ999	Δ417, Δ999	Δ417, Δ999	Δ417, Δ999	Δ417, Δ999	Δ417, Δ999	Δ417, Δ999	Δ417, Δ999	Δ417	Δ999
Infection ^d	–	–	–	–	–	–	+	+	–	–
RT-PCR of RNA from infection supernatants ^e	ND	ND	ND	ND	ND	ND	Δ417, Δ999	Δ417, Δ999, <i>st</i> ^f	ND	ND

^a Construction of plasmids containing genomes with deletions Δ417 and Δ999 (pMTΔ417 and pMTΔ999, respectively), in vitro transcription, and BHK-21 cell transfection are described in Materials and Methods. Boldface type indicates the presence of complementation of defective RNAs.

^b Cytopathology of 10⁶ cells at the indicated times posttransfection; +, >90% cell killing; –, no detectable cytopathology. In transfections with about 500 ng of an RNA transcript of plasmid pMT28 (standard C-S8c1 RNA, described in Materials and Methods) complete cytopathology is observed between 48 and 72 h posttransfection; the equivalent time for O₁K transcripts was about 12 h.

^c The amplifications used were numbers 10, 17, and 21 (Fig. 1A) and 29 (Table 1). At 5 days posttransfection, Δ417 and Δ999 RNA levels in the cotransfection supernatants were about 1.0 × 10⁴ molecules of RNA per cell, versus 1.4 × 10⁴ at time zero after coelectroporation (determined by real-time PCR) (see Materials and Methods). In transfections with Δ999 alone, the amount of RNA was about 7 × 10¹ molecules per cell at 5 days posttransfection, versus 5 × 10³ molecules per cell at time zero after electroporation.

^d Infection of 10⁴ BHK-21 cells with the supernatant obtained at different times posttransfection is indicated. +, >90% cell killing; –, no detectable cytopathology.

^e The amplifications used were numbers 10, 17, and 21 (Fig. 1A) and 29 (Table 1); ND, not determined.

^f Sequence analysis revealed that the standard (st) RNA probably arose by recombination of Δ417 and Δ999 RNAs (data not shown; see Discussion).

of transfected cells (see Discussion). In contrast, at 5 days after cotransfection with a mixture of Δ417 and Δ999 RNAs, cytopathology of the electroporated cells was observed and only RNAs Δ417 and Δ999 were detected. At 72 h after cotransfection, although no cytopathology was yet observed, the supernatant of BHK-21 cells cotransfected with Δ417 and Δ999 RNAs produced cytopathology at 5 days postinfection of fresh BHK-21 cells. Again, only Δ417 and Δ999 RNAs were detected as progeny RNAs. Thus, Δ417 and Δ999 RNAs are defective RNAs, and they produce infection by complementation in the absence of standard RNA.

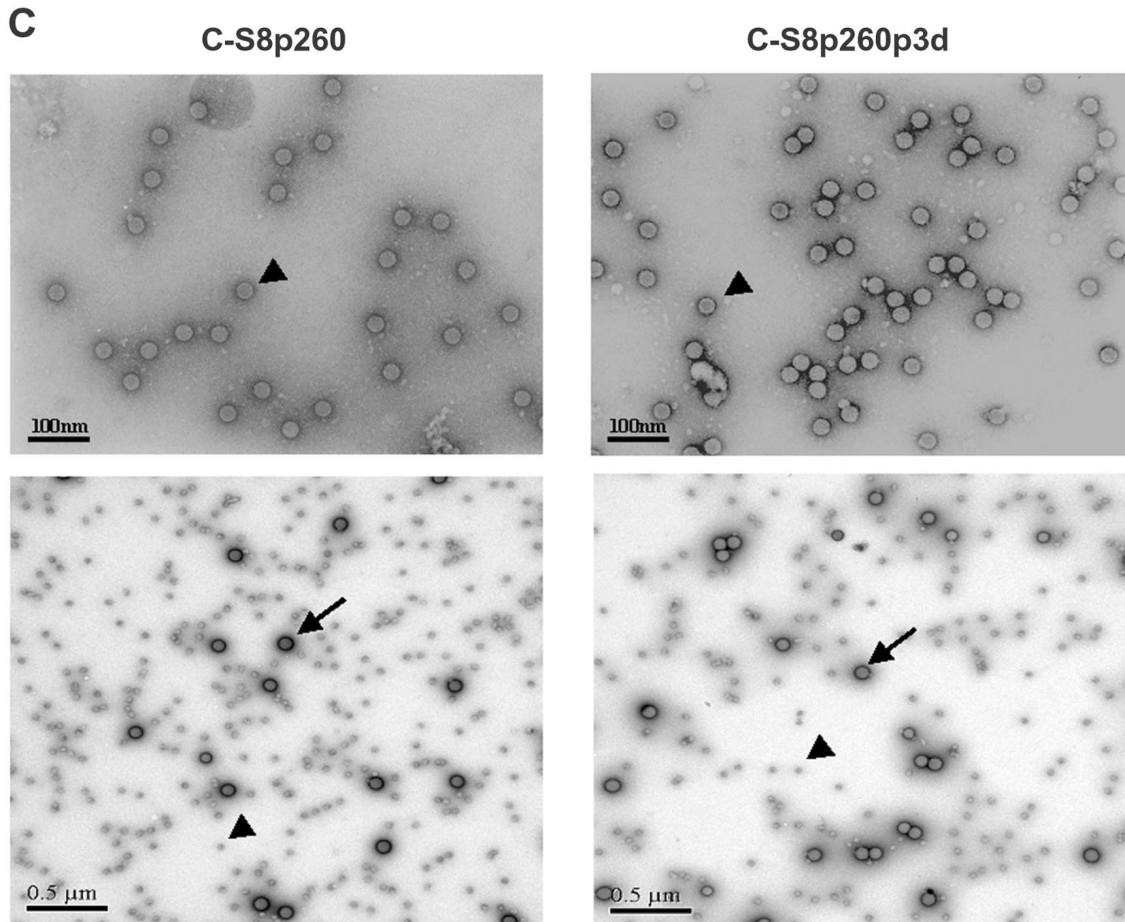
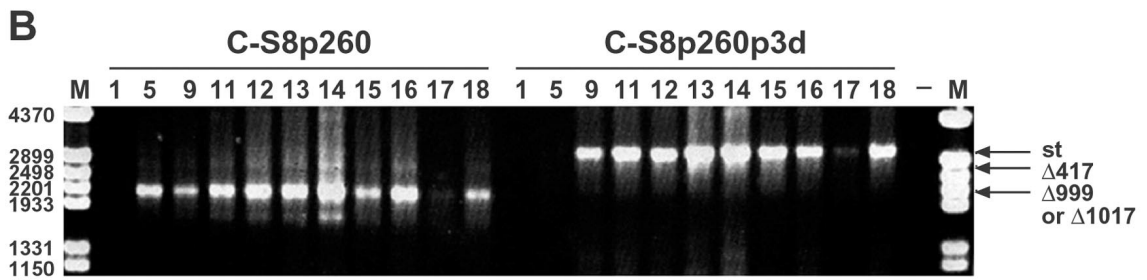
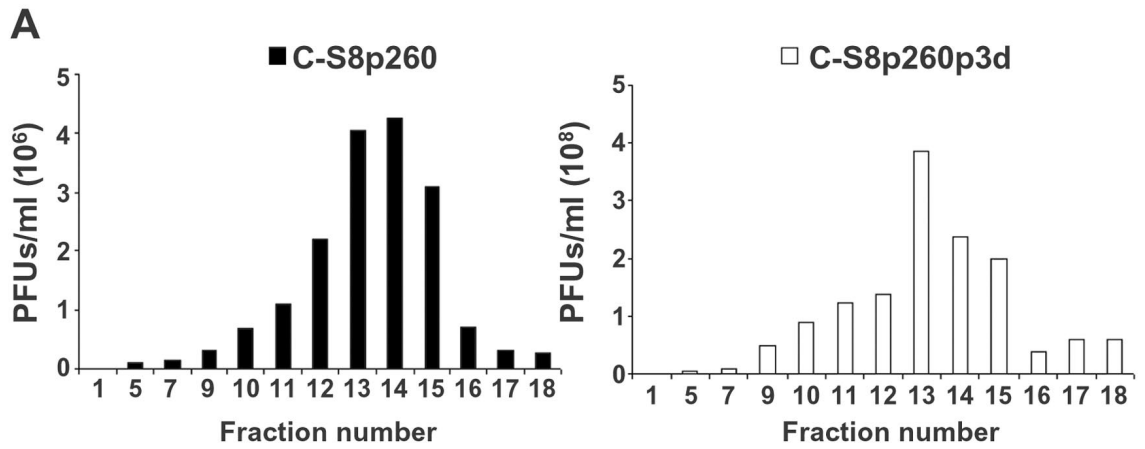
Defective RNAs are encapsidated in particles and each particle contains one defective genome. To determine whether defective RNAs are packaged in viral particles, C-S8p260 and C-S8p260p3d were sedimented through a sucrose gradient, and fractions were analyzed for infectivity and the presence of defective or standard genomes by electron microscopy. Defective RNAs present in C-S8p260 and standard RNA present in C-S8p260p3d comigrated in the sucrose gradient, with maximum infectivity and RNA levels in fractions 13 to 15 (Fig. 3A and B). Electron microscopy examination showed that both populations contained particles of 30 ± 0.1 nm in diameter (Fig. 3C). To determine whether one particle contained one or

more defective RNA molecules, the amount of RNA in C-S8p260 (determined by real-time PCR), was compared with the number of particles (calculated by quantitative electron microscopy) (Fig. 3C). The values obtained were 3.6 ± 1.6 × 10⁸ RNA molecules/μl and 5.5 ± 0.8 × 10⁸ viral particles/μl for C-S8p260 and 9.5 ± 0.8 × 10⁸ RNA molecules/μl and 1.5 ± 0.6 × 10⁹ viral particles/μl for C-S8p260p3d (average of 3 to 10 determinations). Therefore, in C-S8p260 each viral particle contains one defective RNA molecule, and in C-S8p260p3d each viral particle contains one standard RNA genome. We conclude that FMDV evolved in cell culture to produce a population dominated by virus particles containing defective RNAs that were infectious by complementation.

DISCUSSION

Defective viral genomes requiring a helper virus for replication are frequently generated upon serial high MOI passage of RNA viruses (14–16, 29, 32, 35). Deletions in most picornavirus DI genomes are located in the 5' portion of the viral RNA in the capsid protein-coding region (20, 26), and they ranged between 4 and 16% of the genomic residues (21). Packaging constraints dictate the approximate size limits of genome

FIG. 3. Analysis of encapsidation of viral genomic RNAs from FMDV C-S8p260 and C-S8p260p3d. (A) Sedimentation analysis of C-S8p260 and C-S8p260p3d. Sucrose density gradient infectivity profile of FMDV preparations C-S8p260 and C-S8p260p3d. Viral particles were purified as described in Materials and Methods. Infectivity was measured by titration of each gradient fraction. Fraction 1 corresponds to the top and fraction 18 to the bottom of the gradients. Each value represents the mean of triplicate assays and standard deviations (data not shown) never exceeded 15%. (B) Agarose gel electrophoresis of the products of RT-PCR amplifications of FMDV RNAs extracted from fractions of the sucrose gradient sedimentation of C-S8p260 and C-S8p260p3d. Gradient fractions from which the RNAs were analyzed correspond to those shown in panel A, and the fraction number is indicated above each lane. Amplification 21 (Fig. 1A) was used. Input RNA was diluted 100 times to make it limiting for the amplification reaction so that the amount of PCR product obtained was proportional to the input template RNA. Amplification products corresponding to the standard (st) and to the RNAs with deletions (Δ417 and Δ999 or Δ1017) are shown. Lane M, molecular size markers (HindIII-digested φ29pDNA; the corresponding sizes [base pairs] are indicated on the left); lane –, negative control without RNA. (C) Electron microscopy photographs of viral populations C-S8p260 and C-S8p260p3d. Purified virus from fraction 14 of the sucrose gradients (Fig. 3A) was analyzed by electron microscopy. Negatively stained viral particles (examples indicated by arrowheads) at a magnification of ×25,000 (top frames). The measured size of the viral particles in both populations was 30 ± 0.1 nm (average of 30 measurements). Photographs of viral particles (examples indicated by arrowheads) mixed with 91-nm latex beads (examples indicated by arrows) of known size and concentration at a magnification of ×8,000 (bottom frames). C-S8p260 was not diluted; C-S8p260p3d was diluted 5 times; latex beads were diluted 20 times in both cases. Methods are detailed in Materials and Methods.



deletions that can be accommodated by viral encapsidation mechanisms (14, 35). In the case of FMDV, defective $\Delta 417$ RNA—lacking 417 nucleotides of the L region—was shown to be packaged and to contribute capsid proteins to the particles of the helper virus (6). Engineered FMDV RNA lacking the complete open reading frame of protein Lb produced infectious virus upon transfection of BHK-21 cells (30). O₁K FMDV RNA transcripts lacking Lb- and capsid-coding regions were replication competent but their *trans* encapsidation upon superinfection with homologous virus was inefficient (22). The difference between this O₁K-based replicon and the defective RNAs described here in their capacities to produce cytopathology may be influenced by nucleotide sequence context, the nature of the deletions, or a longer time required for cytopathology in transfections with C-S8c1 cDNA transcripts than with O₁K cDNA transcripts (Table 3). The observed complementation between FMDV-defective genomes lacking the L protease and some capsid proteins is in agreement with the *trans*-acting properties of these proteins (22, 23, 30, 39).

Engineered RNAs encoding nonstructural or structural proteins of Sindbis virus could function to produce infectious particles with copackaged bipartite RNA (13). DI RNAs of mouse hepatitis virus could complement engineered RNAs expressing the missing proteins (18). In the DNA virus simian virus 40, a defective DNA encoding mostly early functions could complement another defective DNA encoding late functions to produce infectivity (27). Both DNAs contained iterated replication origins that could contribute to their stability and infectivity.

In the present study we have documented that FMDV can evolve to produce defective genomes that can replicate and kill cells in the absence of wild-type virus. This has been shown by independent procedures such as the presence of defective genomes in individual viral plaques, infection by transcripts of the defective genomes, and two-hit kinetics for cell killing.

What could trigger the evolutionary transition from a high fitness, replication-competent standard FMDV genome toward two RNA forms with deletions that become dominant and are infectious by complementation? Theoretical studies have led to two main proposals for the driving force for genome segmentation. One proposal is that genome segmentation evolved in response to high mutation rates to provide multicomponent reproduction as a form of sex to attenuate the effect of deleterious mutations (5, 31). In this respect, it has been recently reported that genomes of nucleopolyhedrovirus with deletions can work with full-length partners to mutual benefit, possibly through complementation (19). Another proposal is that segmentation could result from selection of shorter RNA molecules that replicate faster than the corresponding parental genome, favored at high MOIs to ensure efficient complementation (25, 40). Deleted forms of viral RNAs have indeed been shown to have a selective replicative advantage over parental full-length genomes *in vitro* (24, 34). A difference of replication capacity or of tolerance to mutations is now amenable to direct experimental testing with the segmented-unsegmented FMDV genome system, and such experiments are currently in progress.

Nucleotide sequence analyses (unpublished data) suggest that a recombination event within the VP4-coding region could be involved in the transition from the segmented to the unseg-

mented FMDV genome, a transition which is strongly selected at low MOIs.

It is not possible to know the relevance of these observations in cell culture for the natural evolution of RNA genomes or whether in nature segmented RNA genomes evolved from or preceded unsegmented forms. What our results show, however, is that RNA genomes have an evolutionary potential to evolve towards genome segmentation within infected cells, provided a strong selective pressure to favor complementation (high MOI) is present. A number of plant RNA viruses have segmented genomes encapsidated into separate particles (multipartite genomes) (43). The FMDV provides an experimental system with which to compare possible advantages of segmentation in ways that have not been possible until now because segmented and unsegmented cognate forms can be compared. It will be also intriguing to examine further the evolution of the system dominated by defective RNAs at high MOI passage and to analyze whether additional divergence and functional specialization of the two segments occur. These studies may be relevant for probing the advantage of sex in genetic systems.

ACKNOWLEDGMENTS

We are indebted to J. J. Holland for valuable suggestions, to M. T. Rejas for the electron microscopy analysis, and to M. Dávila for able technical assistance.

This work was supported by grant BMC2001.1823 C02-01 from MCyT and grant QLRT-2001-00825 from the EU and Fundación Ramón Areces. J.G.-A. was supported by a predoctoral fellowship from MSyC.

REFERENCES

1. **Alberts, B., A. Johnson, J. Lewis, M. Raff, K. Roberts, and P. Walter.** 2002. Molecular biology of the cell. Garland Science, New York, N.Y.
2. **Baranowski, E., C. M. Ruiz-Jarabo, and E. Domingo.** 2001. Evolution of cell recognition by viruses. *Science* **292**:1102–1105.
3. **Baranowski, E., N. Sevilla, N. Verdagué, C. M. Ruiz-Jarabo, E. Beck, and E. Domingo.** 1998. Multiple virulence determinants of foot-and-mouth disease virus in cell culture. *J. Virol.* **72**:6362–6372.
4. **Belsham, G. J.** 1993. Distinctive features of foot-and-mouth disease virus, a member of the picornavirus family; aspects of virus protein synthesis, protein processing and structure. *Prog. Biophys. Mol. Biol.* **60**:241–260.
5. **Chao, L.** 1991. Levels of selection, evolution of sex in RNA viruses, and the origin of life. *J. Theor. Biol.* **153**:229–246.
6. **Charpentier, N., M. Dávila, E. Domingo, and C. Escarmís.** 1996. Long-term, large-population passage of aphthovirus can generate and amplify defective noninterfering particles deleted in the leader protease gene. *Virology* **223**:10–18.
7. **Díez, J., M. Dávila, C. Escarmís, M. G. Mateu, J. Dominguez, J. J. Pérez, E. Giralt, J. A. Melero, and E. Domingo.** 1990. Unique amino acid substitutions in the capsid proteins of foot-and-mouth disease virus from a persistent infection in cell culture. *J. Virol.* **64**:5519–5528.
8. **Domingo, E., C. Biebricher, M. Eigen, and J. J. Holland.** 2001. Quasispecies and RNA virus evolution: principles and consequences. Landes Bioscience, Austin, Tex.
9. **Domingo, E., M. Dávila, and J. Ortín.** 1980. Nucleotide sequence heterogeneity of the RNA from a natural population of foot-and-mouth-disease virus. *Gene* **11**:333–346.
10. **Escarmís, C., M. Dávila, N. Charpentier, A. Bracho, A. Moya, and E. Domingo.** 1996. Genetic lesions associated with Muller's ratchet in an RNA virus. *J. Mol. Biol.* **264**:255–267.
11. **Escarmís, C., M. Dávila, and E. Domingo.** 1999. Multiple molecular pathways for fitness recovery of an RNA virus debilitated by operation of Muller's ratchet. *J. Mol. Biol.* **285**:495–505.
12. **Flint, S. J., L. W. Enquist, V. R. Racaniello, and A. M. Skalka.** 2004. Principles of virology: molecular biology, pathogenesis, and control of animal viruses, 2nd ed. ASM Press, Washington, D.C.
13. **Geigenmüller-Gnirke, U., B. Weiss, R. Wright, and S. Schlesinger.** 1991. Complementation between Sindbis viral RNAs produces infectious particles with a bipartite genome. *Proc. Natl. Acad. Sci. USA* **88**:3253–3257.
14. **Holland, J. J.** 1990. Defective viral genomes, p. 151–165. *In* B. M. Fields, D. M. Knipe, R. M. Chanock, M. S. Hirsch, J. L. Melnick, T. P. Monath, and B. Roizman (ed.), *Fields virology*, 2nd ed. Raven Press, New York, N. Y.

15. **Huang, A., and D. Baltimore.** 1977. Defective interfering animal viruses, p. 73–106. *In* H. Fraenkel-Conrat and R. R. Wagner (ed.), *Comprehensive virology*. Plenum Press, New York, N.Y.
16. **Huang, A. S.** 1973. Defective interfering viruses. *Annu. Rev. Microbiol.* **27**:101–117.
17. **Jackson, T., F. M. Ellard, R. A. Ghazaleh, S. M. Brookes, W. E. Blakemore, A. H. Corteyn, D. I. Stuart, J. W. Newman, and A. M. King.** 1996. Efficient infection of cells in culture by type O foot-and-mouth disease virus requires binding to cell surface heparan sulfate. *J. Virol.* **70**:5282–5287.
18. **Kim, K. H., K. Narayanan, and S. Makino.** 1997. Assembled coronavirus from complementation of two defective interfering RNAs. *J. Virol.* **71**:3922–3931.
19. **López-Ferber, M., O. Simon, T. Williams, and P. Caballero.** 2003. Defective or effective? Mutualistic interactions between virus genotypes. *Proc. R. Soc. Lond. B* **270**:2249–2255.
20. **Lundquist, R. E., M. Sullivan, and J. V. Maizel, Jr.** 1979. Characterization of a new isolate of poliovirus defective interfering particles. *Cell* **18**:759–769.
21. **McClure, M. A., J. J. Holland, and J. Perrault.** 1980. Generation of defective interfering particles in picornaviruses. *Virology* **100**:408–418.
22. **McInerney, G. M., A. M. King, N. Ross-Smith, and G. J. Belsham.** 2000. Replication-competent foot-and-mouth disease virus RNAs lacking capsid coding sequences. *J. Gen. Virol.* **81**:1699–1702.
23. **Medina, M., E. Domingo, J. K. Brangwyn, and G. J. Belsham.** 1993. The two species of the foot-and-mouth disease virus leader protein, expressed individually, exhibit the same activities. *Virology* **194**:355–359.
24. **Mills, D. R., R. L. Peterson, and S. Spiegelman.** 1967. An extracellular Darwinian experiment with a self-duplicating nucleic acid molecule. *Proc. Natl. Acad. Sci. USA* **58**:217–224.
25. **Nee, S.** 1987. The evolution of multicompartmental genomes in viruses. *J. Mol. Evol.* **25**:277–281.
26. **Nomoto, A., A. Jacobson, Y. F. Lee, J. Dunn, and E. Wimmer.** 1979. Defective interfering particles of poliovirus: mapping of the deletion and evidence that the deletions in the genomes of DI(1), (2) and (3) are located in the same region. *J. Mol. Biol.* **128**:179–196.
27. **O'Neill, F. J., E. B. Maryon, and D. Carroll.** 1982. Isolation and characterization of defective simian virus 40 genomes which complement for infectivity. *J. Virol.* **43**:18–25.
28. **Pariente, N., S. Sierra, P. R. Lowenstein, and E. Domingo.** 2001. Efficient virus extinction by combinations of a mutagen and antiviral inhibitors. *J. Virol.* **75**:9723–9730.
29. **Perrault, J.** 1981. Origin and replication of defective interfering particles. *Curr. Top. Microbiol. Immunol.* **93**:151–207.
30. **Piccone, M. E., E. Rieder, P. W. Mason, and M. J. Grubman.** 1995. The foot-and-mouth disease virus leader proteinase gene is not required for viral replication. *J. Virol.* **69**:5376–5382.
31. **Pressing, J., and D. C. Reaney.** 1984. Divided genomes and intrinsic noise. *J. Mol. Evol.* **20**:135–146.
32. **Roux, L., A. E. Simon, and J. J. Holland.** 1991. Effects of defective interfering viruses on virus replication and pathogenesis in vitro and in vivo. *Adv. Virus Res.* **40**:181–211.
33. **Rowlands, D. J. (ed.).** 2003. Foot-and-mouth disease. *Virus Res.* **91**:1–161.
34. **Sabo, D. L., E. Domingo, E. F. Bandle, R. A. Flavell, and C. Weissmann.** 1977. A guanosine to adenosine transition in the 3' terminal extracistronic region of bacteriophage Q β RNA leading to loss of infectivity. *J. Mol. Biol.* **112**:235–252.
35. **Schlesinger, S.** 1988. The generation and amplification of defective interfering RNAs, p. 167–185. *In* E. Domingo, J. J. Holland, and P. Ahlquist (ed.), *RNA genetics*. CRC Press, Boca Raton, Florida.
36. **Sevilla, N., and E. Domingo.** 1996. Evolution of a persistent aphthovirus in cytolytic infections: partial reversion of phenotypic traits accompanied by genetic diversification. *J. Virol.* **70**:6617–6624.
37. **Sierra, S., M. Dávila, P. R. Lowenstein, and E. Domingo.** 2000. Response of foot-and-mouth disease virus to increased mutagenesis: influence of viral load and fitness in loss of infectivity. *J. Virol.* **74**:8316–8323.
38. **Sobrinho, F., M. Dávila, J. Ortín, and E. Domingo.** 1983. Multiple genetic variants arise in the course of replication of foot-and-mouth disease virus in cell culture. *Virology* **128**:310–318.
39. **Strebel, K., and E. Beck.** 1986. A second protease of foot-and-mouth disease virus. *J. Virol.* **58**:893–899.
40. **Szathmary, E.** 1992. Natural selection and dynamical coexistence of defective and complementing virus segments. *J. Theor. Biol.* **157**:383–406.
41. **Toja, M.** 1997. Caracterización molecular de un virus de la fiebre aftosa y de sus derivados persistentes. Construcción de un clon infeccioso. Ph.D. thesis. Universidad Autónoma de Madrid, Madrid, Spain.
42. **Toja, M., C. Escarmis, and E. Domingo.** 1999. Genomic nucleotide sequence of a foot-and-mouth disease virus clone and its persistent derivatives. Implications for the evolution of viral quasispecies during a persistent infection. *Virus Res.* **64**:161–171.
43. **van Regenmortel, M. H. V., C. M. Fauquet, D. H. L. Bishop, E. B. Carstens, M. K. Estes, S. M. Lemon, J. Maniloff, M. A. Mayo, D. J. Mc Geoch, C. R. Pringle, and R. B. Wickner (ed.).** 2000. *Virus taxonomy*. Seventh report of the International Committee on Taxonomy of Viruses. Academic Press, San Diego, Calif.